CanmetMATERIALS

Evaluation of Current Tank Car TC128B Steel Weld Performance

S. Xu, J. Chen, J. McKinley, J. Liang, L. Yang and A. Laver

Report No. CMAT-2020-WF 49867504

TP 15470E

March 2020

(Updated February 2021)

CMAT

DISCLAIMER

CanmetMATERIALS

REPORT CMAT-2020-WF 49867504

EVALUATION OF CURRENT TANK CAR TC128B STEEL WELD PERFORMANCE

by

S. Xu, J. Chen, J. McKinley, J. Liang, L. Yang and A. Laver

EXECUTIVE SUMMARY

This report summarizes the results of the evaluation of current TC128B tank car welds. The sample coupons were received from a DOT-117J tank car. The experimental work in this report included the determination, from a longitudinal weld, of (i) chemical composition, microstructure and micro-hardness (ii) tensile strength and failure locations in the temperature range of 23°C to -60°C, and (iii) Charpy transition curves. Typical fracture features of low Charpy weld metal samples and volume fractions of acicular ferrite (AF) were characterized and discussed. The results of the longitudinal weld were compared to those from a circumferential weld characterized previously from the same tank car including updated Charpy testing at -34°C, and the main conclusions are provided in this report.

The TC128B welds were created using a double pass procedure. The first-pass (or root pass) weld was made from the inside of the tank and the Weld Metal (WM) height was about 1/3 of the weld thickness while the second-pass (or cap pass) weld completed the joints. For the two welds, the combined weld and Heat Affected Zone (HAZ) widths were approximately 14.8-19.8 mm close to the mid-thickness (the smallest). The HAZ width ranged approximately 1.3-5.7 mm. WM and HAZ showed typical microstructures although AF volume was low. The hardness values in the weld and HAZ were considerably higher than those of Base Metal (BM), i.e., demonstrating desired weld strength over-matching. The hardness values of the two welds were comparable. The average values of micro-hardness of BM, HAZ and WM of the two welds were 164, 191 and 201, respectively. All-WM specimens tested at 23°C showed that the welds were manufactured to the required strength specification and the welds were stronger than the steel. The Ultimate Tensile Strength (UTS) of the cross-weld specimens decreased with increasing temperature from -60°C to 850°C. All cross-weld specimens tested failed at BM except for two cross-weld tensile specimens at 800°C failed at WM indicating that the weld overmatched (stronger than) the BM. Charpy V Notch (CVN) values of WM were significantly lower than those of BM and HAZs specimens. Interpolated CVN values for circumferential WM specimens at -34°C (average 18 J) indicated that the weld toughness values may be lower than the benchmark of AAR specification requirements for pressure tank (i.e., average 20.3 J). Additional Charpy tests (3) and a retest (of 3) at -34°C showed that the toughness of the circumferential weld were lower than the bench requirements (i.e., average of 20.3 J and minimum of 13.6 J). The results indicate that Charpy testing is important for tank cars in low-temperature climate applications. The Scanning Electron Microscopy (SEM) fractography examinations indicate that low TC128B WM toughness was associated with weld microstructural constituents and/or inclusions. The volume fractions of AF in the circumferential and longitudinal welds were estimated to be 25% and 40%, respectively.

CONTENTS

1. INTRODUCTION

Welding techniques are utilized in the manufacturing of tanks cars. Mechanical properties of tank car steel and welds are critical to the integrity of the tank car. In recent work funded by Transport Canada [1-3], steel and circumferential weld samples from a current DOT-117J tank car made of TC128B steel were characterized and evaluated at CanmetMATERIALS. In 2015, the DOT-117 unpressurized tank car was announced as a safety improvement over the existing tank cars to improve safety.

Based on work in [1-3], the TC128B was Carbon-Manganese (C-Mn) steel with vanadium (V) microalloying in normalized condition. The steel had a ferrite and pearlite in a heavily banded structure and had equiaxed grains with grain size approximately 10-20 μm. The circumferential weld was produced by submerged-arc welding with a double pass procedure. The weld metal (WM) microstructure at the middle of weld centerline in the second-pass appeared to consist of coarse proeutectoid ferrite along WM solidification direction, AF and/or bainite, and some pearlite. The hardness values in the weld and heat affected zone (HAZ) were considerably higher than those of base metal (BM), i.e., demonstrating desired weld strength over-matching at room temperature. The steel tensile stress-strain curves showed significant discontinuous yielding at 23°C and 200°C. The steel strength decreased and ductility increased up to 800°C. At 23°C, all-weld-metal-tension and cross-weld tensile tests from the circumferential weld displayed discontinuous yielding. Ultimate tensile strength (UTS) of cross-weld tensile specimens dropped sharply beyond 400°C as it did in BM tests. These tensile properties provide data for the tank car pool fire analysis or for the torch fire analysis which are required by the Association of American Railroads (AAR). Toughness represents the impact absorbing capacity of a material. Charpy V-notch (CVN) toughness ductile-to-brittle transition curves of the steel and circumferential weld and fracture toughness of the steel at 23°C were determined. These toughness results are useful for integrity assessments and manufacture process optimization. The work on the circumferential weld demonstrated two notable findings [3]. The first was that the Charpy toughness of the WM measured by the CVN test per ASTM E23 was much lower than the BM and weld heat-affected zone (HAZ). CVN values for the WM specimens were slightly lower than the AAR required values for low-temperature applications [4]. The second finding was that although the weld metal was stronger than the base metal (BM) at most temperatures at and above room temperature, two cross-weld test specimens at 800°C failed at WM, although the UTSs of the specimens were similar no matter where the specimen failure occurred. Hence, it was of practical engineering interest to test other welds from the same tank car or similar tank cars to confirm the findings on low CVN and survey the cross-weld tensile properties at low temperatures. The AAR specification requires a test temperature of -34 °C for pressure tank cars as a benchmark used in this research for Charpy toughness testing (M-1002 Appendix W 12.1.4 [4]), however, the testing scheme for previous work in [3] was modelled after the previous years testing which utilized the -46 °C test point [1]. From the interpolation best fitting, average CVN value for the circumferential WM at -34°C was 18 J and this indicated that the weld toughness values may be lower than the benchmark (i.e., average 20.3 J [4]). Hence, it was highly desired to have tests of the TC128B welds at -34 °C and compare the results with the CVN requirements.

In this work, additional Charpy tests (3 samples) and a retest (of 3 samples) at -34°C of the circumferential weld was performed. A longitudinal weld from the same DOT-117 tank car made of TC128B steel as used in previous work [1-3] was evaluated and the results were compared with those of the circumferential weld in [3] and in current work when possible. The experimental work consisted of (i) characterization of weld microstructure and hardness, (ii) measurement of Charpy transition curve

of the weld, (iii) investigation of TC128B weld tensile properties at temperature range from 23°C to -60°C, and (iv) determination of typical fracture features of low CVN WM samples and volume fractions of AF. Background information of the tank car, TC128B steel, and the circumferential weld referenced in this report can be found in previous studies [1-3].

2. MATERIAL AND EXPERIMENTAL PROCEDURES

The tank car TC128B weld samples donated by the Federal Railroad Administration (FRA) were taken from a new tank car conforming to DOT-117 specifications, and the shell has a nominal thickness between 12.7 mm (1/2″) to 15.9 mm (10/16″). The tank car was fabricated using a submerged arc welding process in 2015 and subjected to a side-impact test in September 2016. The tank car was purchased and the impact test was sponsored by the FRA an agency of the United States Department of Transportation (DOT). The plate rolling direction (RD) is normal to the axis of the tank. The longitudinal weld sections used in this work are shown in Figure 1. Cross-weld tensile specimens were taken transverse to the weld length and along the RD orientation of the steel plate. The steel thickness was approximately 14.8 mm close to the weld.

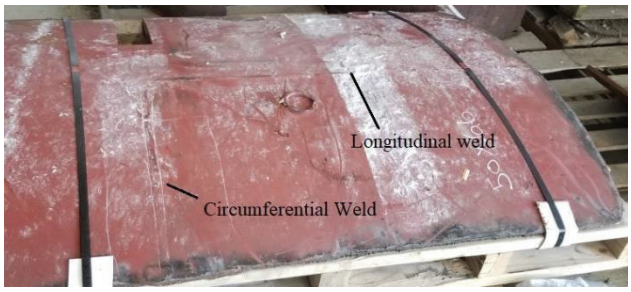

(a) A TC128B section with two welds

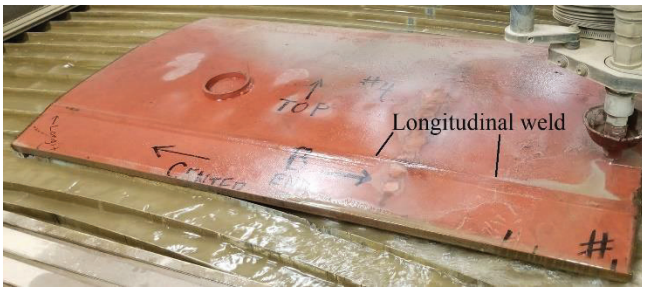

(b) A TC128B weld section on a water-jet machine

Figure 1. Tank car TC128B longitudinal weld samples.

The compositions of the tank car steel (from [1]) and WM samples were analyzed using optical emission spectroscopy and Leco Combustion/Fusion analysis technique for oxygen (O) and nitrogen (N), as are given in Table 1. The chemical composition specifications for the TC128B [4] are listed in Table 1 for reference. The composition meets the ARR 2014 specification for TC128B [4]. The Carbon (C) content of longitudinal weld was considered to be high (typical less than 0.08%) and this is similar to that of the circumferential weld [3]; the Oxygen (O) of the longitudinal weld (0.00559%) was lower than that of the circumferential weld (0.0826%) and slightly higher than typical submerged arc welding (SAW) (~up to 0.05%) [6].

Table 1. Chemical composition of the sample steel [1], limits for TC128B (wt%) [4] and welds

Element	Spectroscopy analysis of BM sample [1]	Spectroscopy analysis of circumferential WM [3]	Spectroscopy analysis of longitudinal WM	TC128B, maximum permitted in product analysis [4]
C	0.19	0.18	0.16	0.26
Mn	1.34	1.54	1.57	1.00-1.70
P	0.0059	0.0182	0.0162	0.025
S	0.0014	0.0117	0.0088	0.009
Si	0.16	0.35	0.41	0.13-0.45
V	0.034	0.016	0.020	0.084
Cu	0.21	0.18	0.19	0.35
Al	0.032	0.021	0.021	0.015-0.060
Nb	<0.001	0.002	-	0.03 (per ASTM A20 [5])
Ti	0.0016	0.0129	0.016	0.020
B	0.0002	0.0004	0.0003	0.0005
O	(Not determined)	0.0826	0.0559	-
N	0.0069	0.00831	0.00625	0.012
Sn	0.0112	0.006	0.0069	0.020
CE*	0.46	0.53	0.53	0.55
Nb+V+Ti	<0.0366	0.031	0.036	0.11
Cu+Ni+Cr+Mo	0.43	0.32	0.36	0.65
Ti/N	0.23	1.6	2.56	4.0

* CE=C+(Mn+Si)/6+(Ni+Cu)/15+(Ni+Mo+V)/5

Transverse weld metallographic specimens with the weld reinforcement were cut using a water-jet machine for microstructural and micro-hardness characterization. Metallography was performed using the standard polishing procedure (final polishing to 0.25 μm diamond paste) and etched using 2% Nital.

Vickers micro-hardness tests were performed using a diamond pyramid indenter with a load of 300 gram-force and a dwell time of 10 seconds. The hardness values (H_v) were measured across the weld at three through-thickness positions: (i) ~2 mm from the tank outside surface; (ii) at the mid-wall thickness; and (iii) ~2 mm from the tank inside surface.

Cross-weld tensile tests were carried out to evaluate the weld performance of DOT-117 tank car made of TC128B steel at different temperatures. Figure 2 shows the cylindrical cross-weld tensile specimen geometry used with a gauge length of 50.8 mm and diameter of 6.25 mm. According to AAR specification [4], the reduced section of cross-weld tension specimens should be longer than the width of weld plus two specimen diameters. The use of this sub-size cylindrical tensile specimen was to facilitate testing at low temperatures and to also allow more specimens for a given length of the weld. Cylindrical tensile specimens were machined from the middle-thickness of the weld. All tests were performed at a quasi-static rate and at temperatures between 23°C and -60°C. Two cylindrical All-Weld-Metal (AWM) specimens with a gauge length of 25.4 mm and diameter of 6.35 mm were taken along the weld close to the middle-thickness to measure WM properties to compare to the specification requirements. Tensile specimens were etched before testing to help examine weld and failure locations. Photo of one AWM and one cross-weld tensile etched specimens are shown in Figure 3.

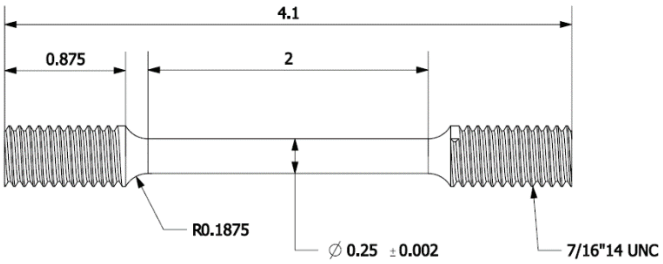

Figure 2. Cylindrical tensile specimen. Dimensions in inch.

Figure 3. Etched AWM and cross-weld tensile specimens of TC128B longitudinal weld.

Full-size CVN specimens were prepared from the circumferential [3] and longitudinal welds according to AAR specification [4]. Charpy specimen location and orientation for tank car WM and HAZ are shown in Figure 4 [4]. Charpy specimen notch was placed through-thickness. Machined Charpy specimens were etched to examine and ensure notch location. Examples of Charpy notch at weld and HAZs are shown in Figure 5. Two types of HAZ notch locations were used, i.e., notched at HAZs of the second-pass weld (Figure 5b) according to [4] and of the first-pass weld (Figure 5c) to illustrate the effect of HAZ location on CVN.

AAR Specification M-1002 Appendix W (Welding of Tank Car Tanks) specifies requirements of Charpy tests and retests [2] that are to be performed during tank car manufacturing when the tank specification requires Charpy testing. M-1002 does not include provisions for performing Charpy tests on in-service or ex-service welds. The AAR publishes standards on in-service inspection of tank cars, however, discussion of these standards is not included here. In Appendix W 8.1.4.1 Table W.1 [2], minimum CVN value of each of two of three specimens and average of the three specimens is 20.3 J; minimum CVN value of one of the three specimens is 13.6 J. Retesting is allowed with conditions as detailed in Appendix W 8.1.4.2 which states “If the value for more than one specimen is below the minimum value specified for the average of three specimens, or if the value for one specimen, or if the value for one specimen is below the minimum value specified for one of the three specimens (the other two being not less than the minimum value specified for the average of three specimens), a retest of

three additional specimens shall be made, each of which must be equal or exceed the specified minimum value for the average of the three specimens. Such a retest shall be permitted only when the average value of the three specimens equals or exceeds the minimum value specified for one of the three specimens."

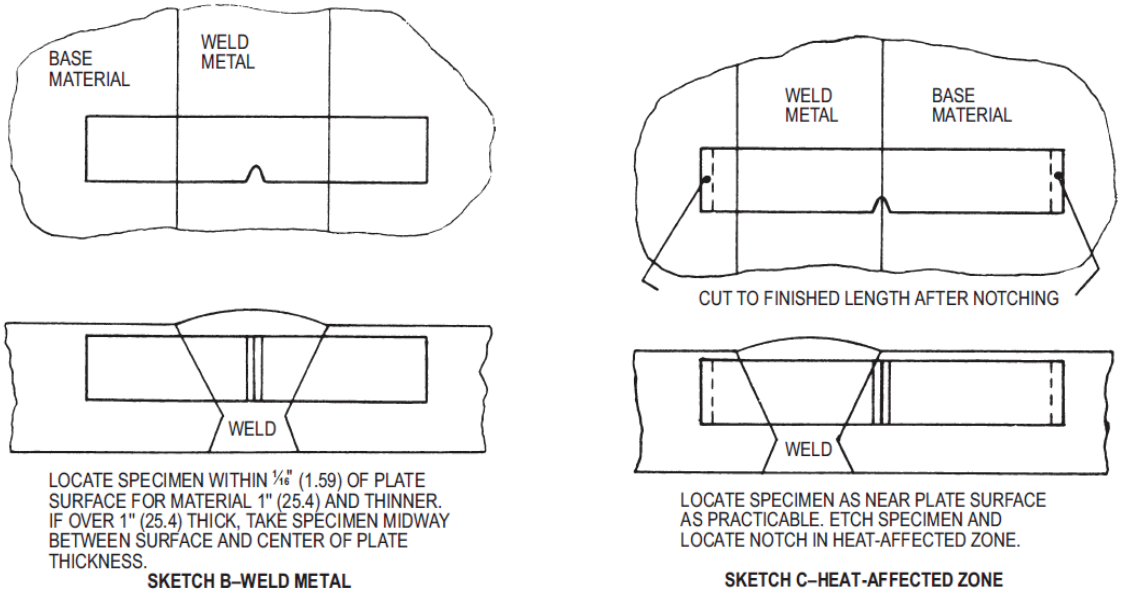

(a) WM (b) HAZ

Figure 4. Charpy specimen location and orientation for tank car WM and HAZ according to AAR specification [4].

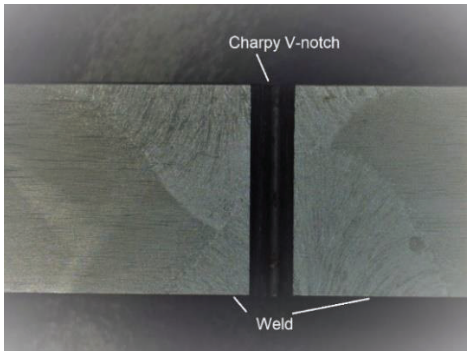

(a) Charpy V-notch at the weld

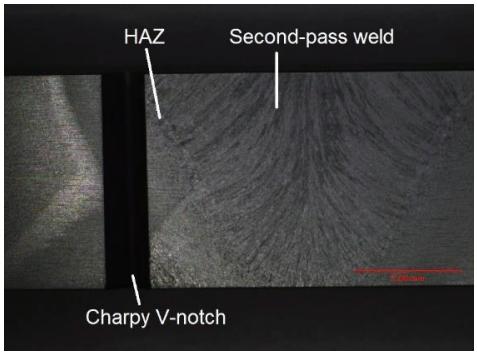

(b) Charpy V-notch at HAZ of the second-pass weld

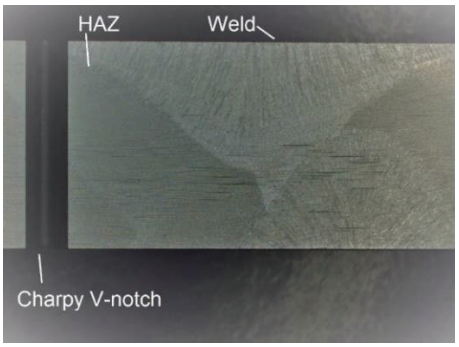

(c) Charpy V-notch at HAZ of the first-pass weld

Figure 5. Photo of Charpy notch location at the weld and HAZ of TC128B longitudinal weld.

Fracture surfaces of two TC128B circumferential WM Charpy specimens tested previously in [3] were examined using a scanning electronic microscope (SEM). Quantitative image analysis was carried out to determine AF volume fraction in WM samples.

3. RESULTS AND DISCUSSION

In order to examine general characteristics of the TC128B longitudinal weld, and assist mechanical specimen preparation, metallography, micro-hardness, and micrography were performed and are described first. Mechanical properties of the longitudinal weld were evaluated and are compared to those of the BM and circumferential weld when possible.

3.1 Macrography of Weld

A macrography of current TC128B manufactured longitudinal weld is shown in Figure 6. The macrography indicates that the weld was produced with a double pass SAW procedure[1], which is a standardized mechanized welding procedure for TC128B tank cars [7]. The first-pass (or root pass) weld was made from the inside of the tank and the WM height was about 1/3 of the weld thickness while the second-pass (or cap pass) weld completed the joining. The first-pass and second-pass welds were not aligned as well as the circumferential weld from the same tank car [3]. The combined weld and HAZ widths were approximately 19.8 mm close to the mid-thickness (the smallest), 25.5 mm at the inside surface and 24.2 mm at the outside surface, respectively. The HAZ width range was approximately 1.3-5.7 mm. There was a doubly tempered HAZ between the first-pass and second-pass WMs in the weld overlap region which is the lightly gray region in Figure 6; this reheated (RH) WM region was, as expected, significantly influenced by the re-heating of the second-pass weld as will be shown in micrographs in Subsection 3.3. The height of the RH WM zone is approximately 1.5 mm at the centerline and the height of the weld was approximately 18.1 mm. The RH WM is approximately 8% of WM. The bay region indicated in Figure 6 will be discussed in the next two subsections.

[1] A submerged arc weld procedure was used to fabricate the tank car.

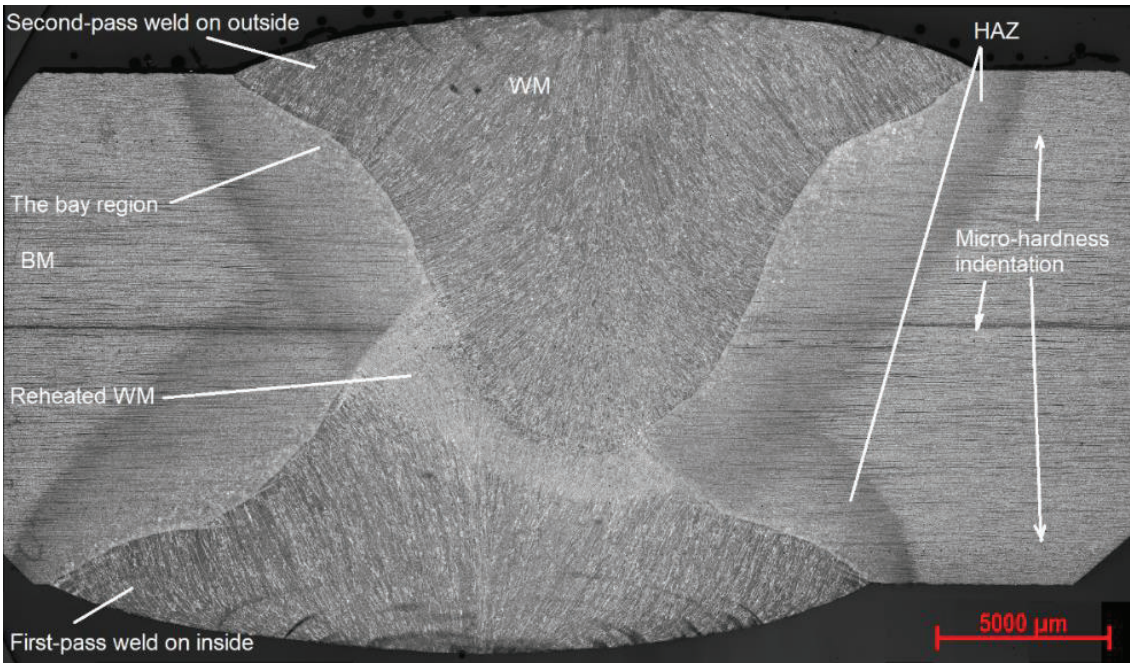

Figure 6. Macrography of TC128B longitudinal weld.

3.2 Micro-hardness Across the Weld Joint

Micro-hardness measurements were made across the weld joint and through-thickness at the weld centerline. The through-thickness measurement started at the center of the second pass (outside) and it was off-center at the first weld. The hardness indentations positions cross the weld are indicated in Figure 6 (although many hardness indentations could not be seen well at this magnification). Micro-hardness measurements are shown in Figure 7 and the average hardness of BM (164) as determined in [3] is shown as a horizontal dash-line for comparison. The regions of BM, HAZ and WM were illustrated in Figure 7a-c based on the indentation locations in Figure 6. The origin of the X-axis in Figure 7 corresponded to the first hardness measurement on the right side in Figure 6. Since the fusion line and HAZ boundaries at the three through-thickness positions are different these boundaries in Figure 7d are not illustrated. The average and standard deviation of micro-hardness (H_v) of HAZ as measured in three through-thickness positions were 190±21 (from 153 to 231) and these of WM were 206±12 (from 158 to 238). The highest hardness values (H_v) in the weld and HAZ were 238 and 231, respectively. The average and standard deviation of through-thickness micro-hardness (H_v) at WM centerline (Figure 7e) were 207±14 (from 185 to 257). The main observation from the measurements was that the hardness values (H_v) in the weld and HAZ were generally considerably higher than those of BM, i.e., demonstrating desired weld strength over-matching. The hardness values (H_v) in the HAZ at 2 mm below the outside surface close to the second-pass weld fusion line (so-called the bay region in Figure 6) were slightly higher than those in the other two thickness positions (Figure 7d). It is typical in SAW welding that the bay region close to the fusion line in the final weld pass usually displays a coarse-grained microstructure (e.g., [8]). The microhardness values (H_v) of the longitudinal weld were comparable to those of the circumferential weld.

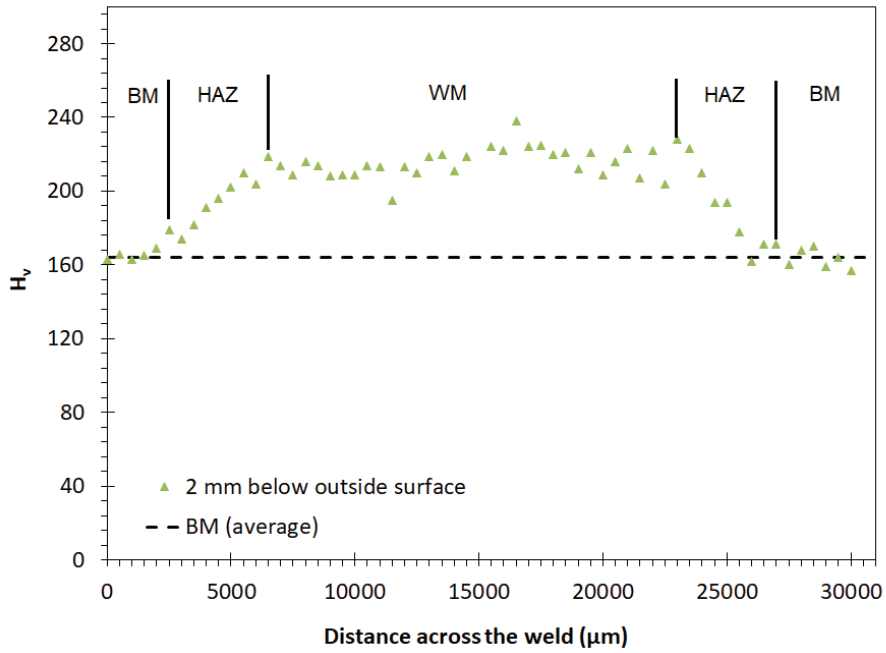

(a) Micro-hardness measured at 2 mm below the outside surface

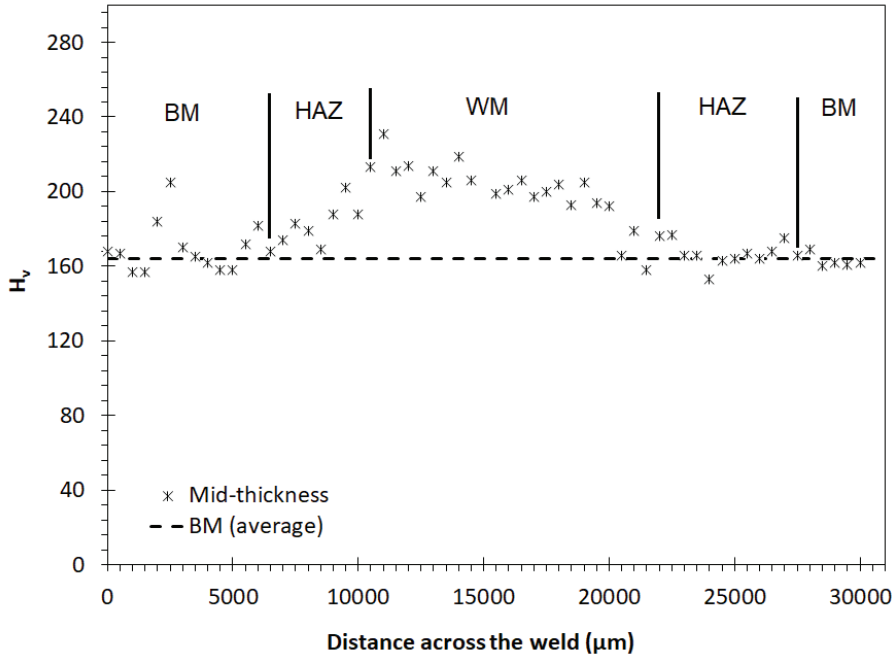

(b) Micro-hardness measured at mid-thickness

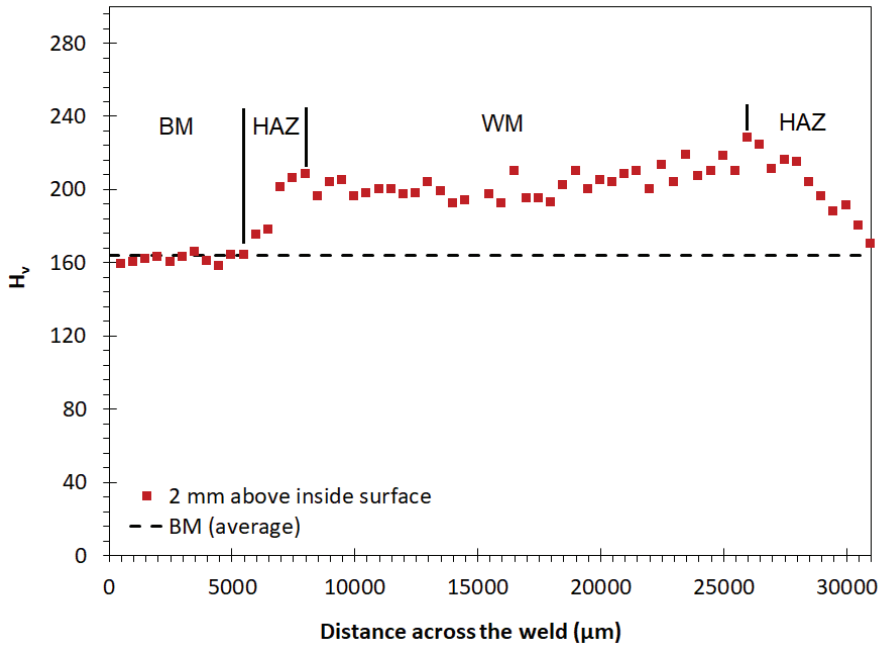

(c) Micro-hardness measured at 2 mm above inside surface

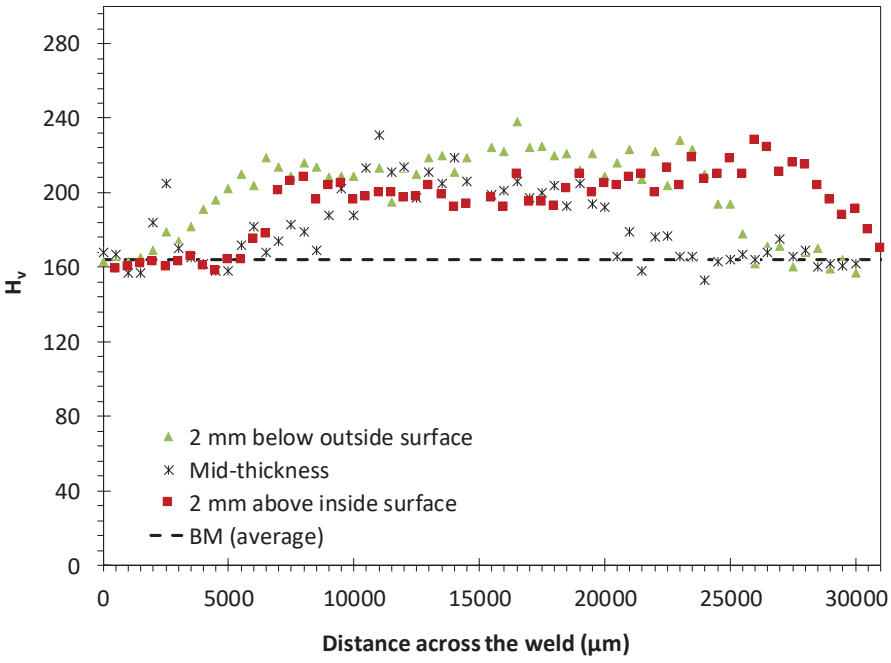

(d) Combined micro-hardness profile

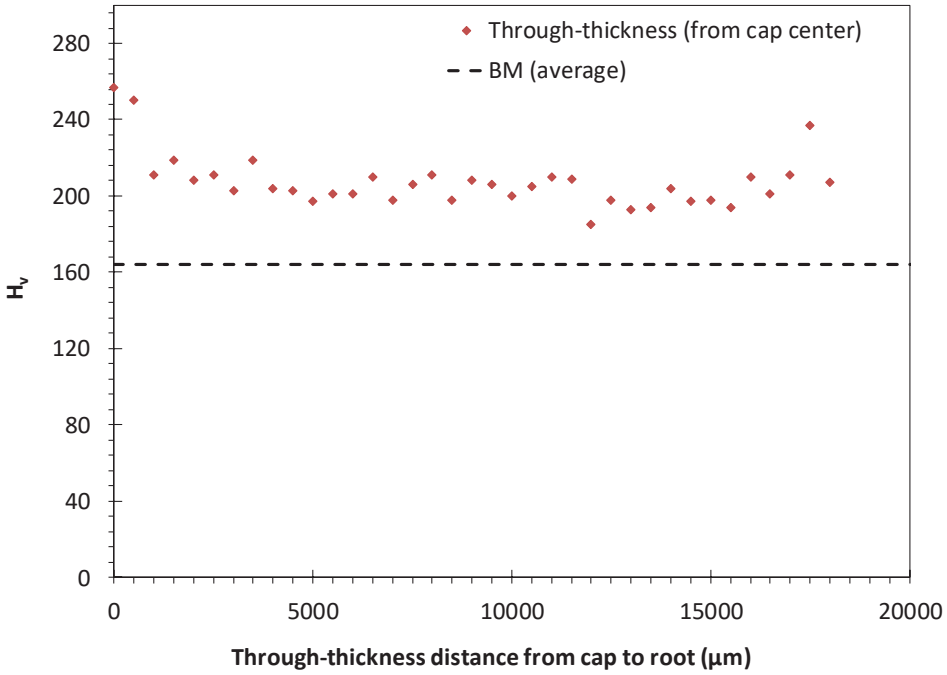

(e) Through-thickness micro-hardness starting from weld cap centerline

Figure 7. Micro-hardness across the TC128B longitudinal weld.

3.3 Microstructure

According to [9,10], the microstructure of HAZ includes (i) coarse grain region (CGHAZ): Material near the fusion boundary that reaches a temperature well above A_{c3} during welding, (ii) fine grain region (FGHAZ): Away from the fusion boundary where the peak temperature is lower, but still above A_{c3}, (iii) intercritical region (ICHAZ): In this regions, peak temperature is between A_{c1} and A_{c3}, resulting in partial reversion to austenite on heating, and (iv) over tempered region. Also noted that since 1998, AAR specification (M-128) requires new tank cars to be stress relieved at 649°C (1200°F) for one hour after fabrication (as cited in [11]). The stress-relieving treatment slightly decreases the strength, increases or maintains the ductility of TC128B and are beneficial to low-temperature fracture properties [12]. As such, the microstructures presented were taken from the weld and HAZ of TC128B after stress-relieving treatment.

The microstructure in the weld joint is more complex than that of the BM. The WM microstructure close to the middle part of the weld centerline in the second-pass is shown in Figure 8. It consisted of coarse pro-eutectoid ferrite (white) along WM solidification direction, AF and/or bainite (grey), and some pearlite (dark). The formation of pearlite in the weld metal indicated that the cooling rate after welding was relatively small. As a result, a very coarse proeutectoid ferrite was formed with a relatively high volume percentage, whereas the volume percentage of AF was small. Low AF volume fraction is usually associated with low toughness which will be discussed later.

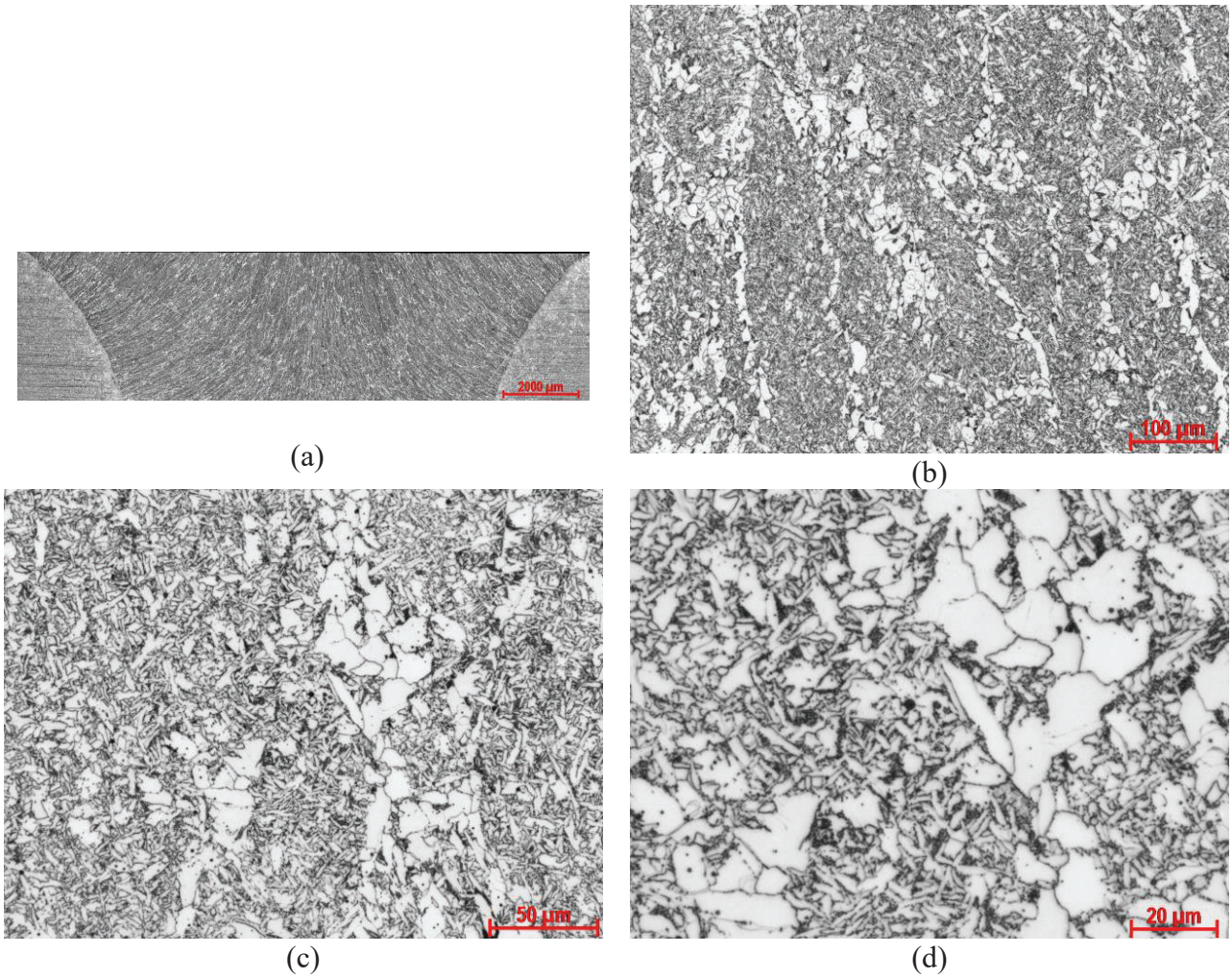

(a) (b)

(c) (d)

Figure 8. Microstructure of TC128B longitudinal WM at the middle of weld centerline in the second-pass.

In the CGHAZ region close to the bay region as shown in Figure 9, coarse grain boundary ferrite was present at prior austenite grain boundaries formed during welding, and within austenitic grains, some Widmanstätten ferrite and AF and/or tempered bainite and/or tempered martensite were observed.

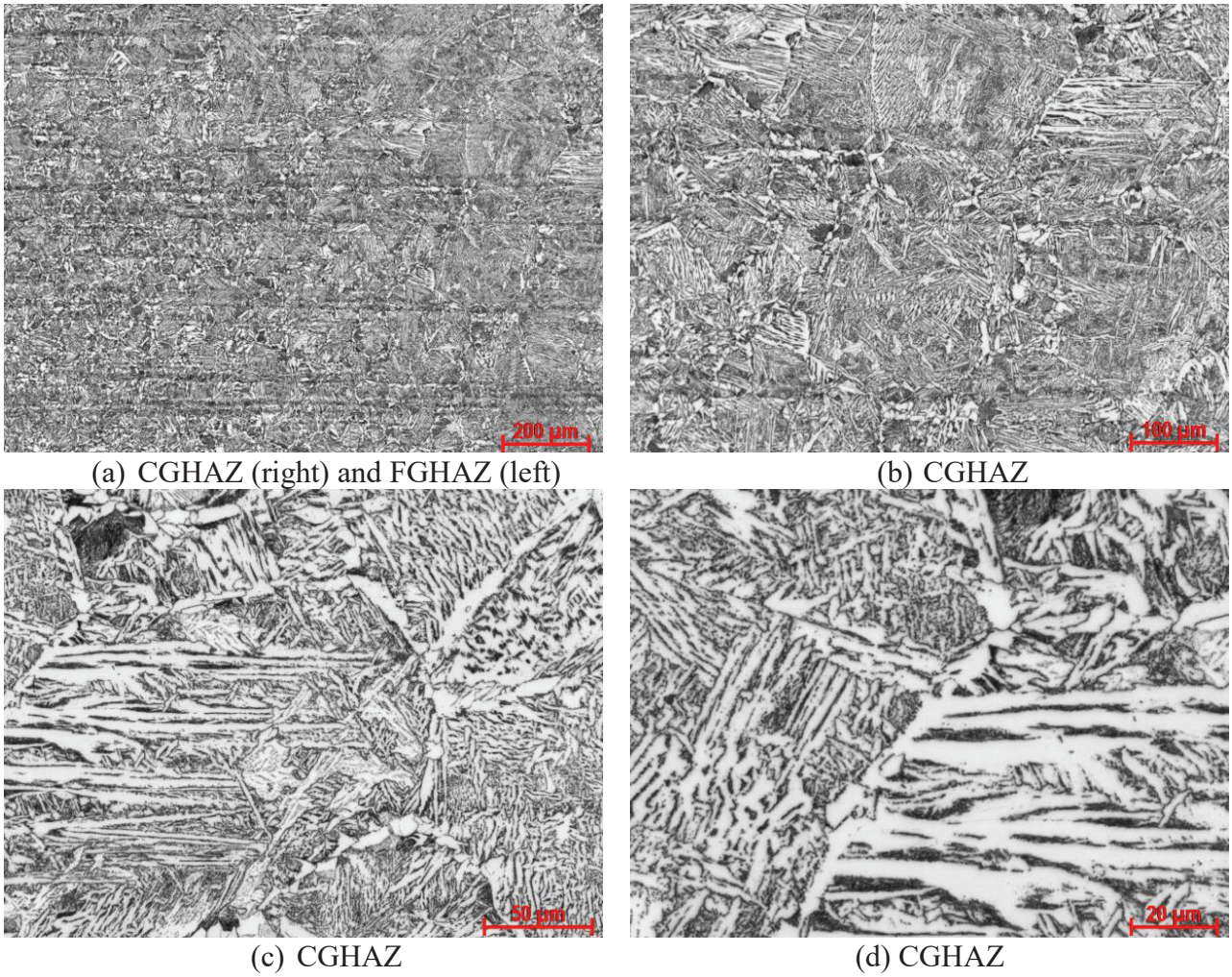

(a) CGHAZ (right) and FGHAZ (left)

(b) CGHAZ

(c) CGHAZ

(d) CGHAZ

Figure 9. Microstructures of CGHAZ.

The transition region of the FGHAZ and ICHAZ is displayed in Figure 10a. Microstructures of the FGHAZ (Figure 10b, Figure 10c and Figure 10d) region close to the mid-thickness of the weld region consisted of fine equiaxed ferrite grains (white), pearlite (dark) and possibly a small amount of bainite, martensite, and retained austenite (grey).

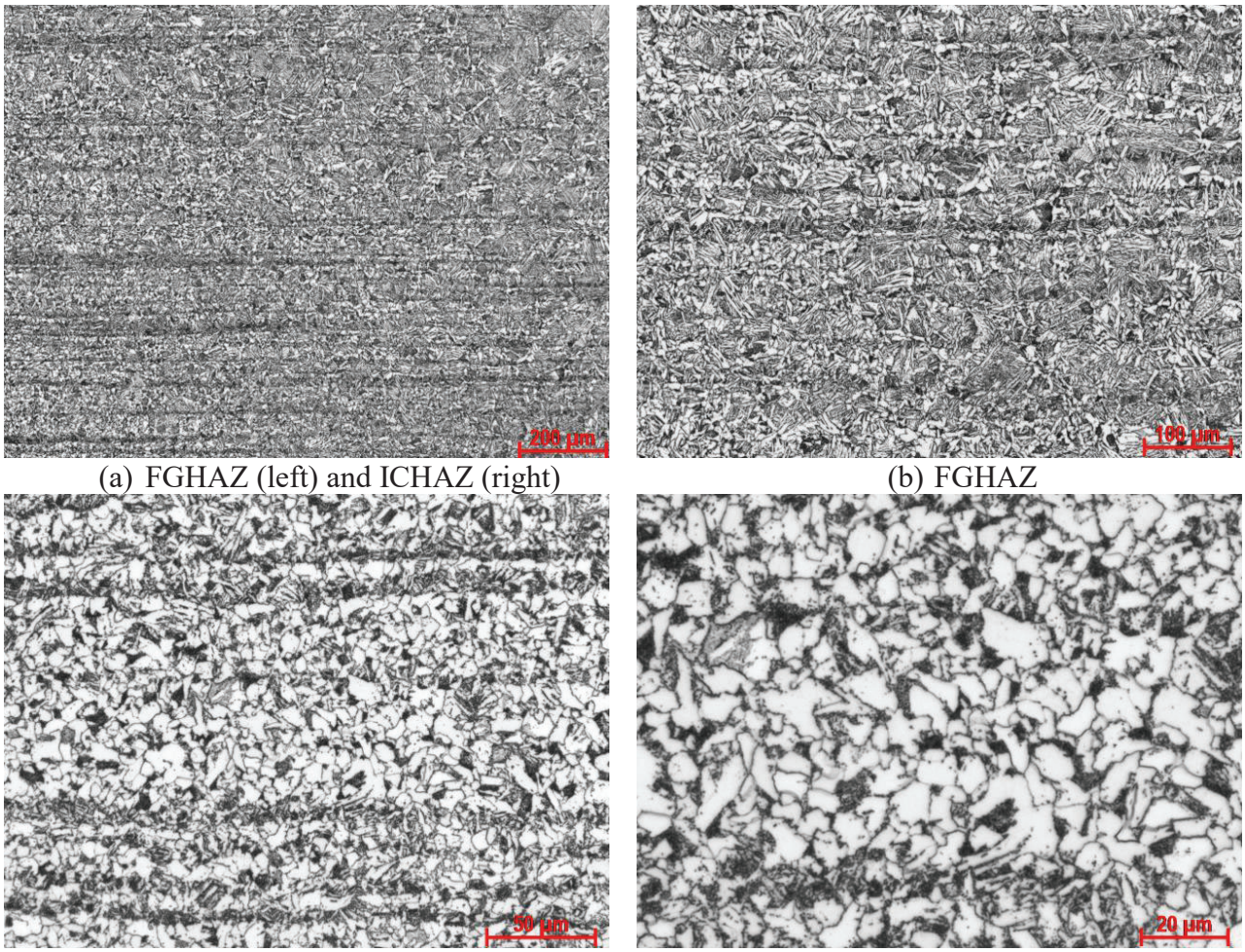

(a) FGHAZ (left) and ICHAZ (right)

(b) FGHAZ

(c) FGHAZ

(d) FGHAZ

Figure 10. Microstructures of FGHAZ close to mid-thickness of the weld region.

The transition region of the FGHAZ and ICHAZ is displayed in Figure 11a. Pearlite bands were similar to those observed in base steel [1,3]. Microstructure of ICHAZ (Figure 11b, Figure 11c and Figure 11d) region close to the mid-thickness of the weld region consisted of fine equiaxed ferrite grains (white) and pearlite (dark).

In summary, the microstructure of both WM and HAZ showed the typical feature of C-Mn steel associated with SAW that was similar to that of the circumferential weld [3]. However, it is worth noting that a very limited volume percentage of AF was formed in the weld metal and very significant austenite grain growth occurred in the CGHAZ region, which indicated that SAW was carried out with relatively high heat input. The volume fraction of AF was found important for good fracture toughness of C-N steel SAW welds [13]. This will be further discussed in section 4.2. The welding procedure specification for manufacturing the tank car needs to be reviewed in order to understand better the relationship between welding parameters, filler alloy composition and microstructure of weld metal.

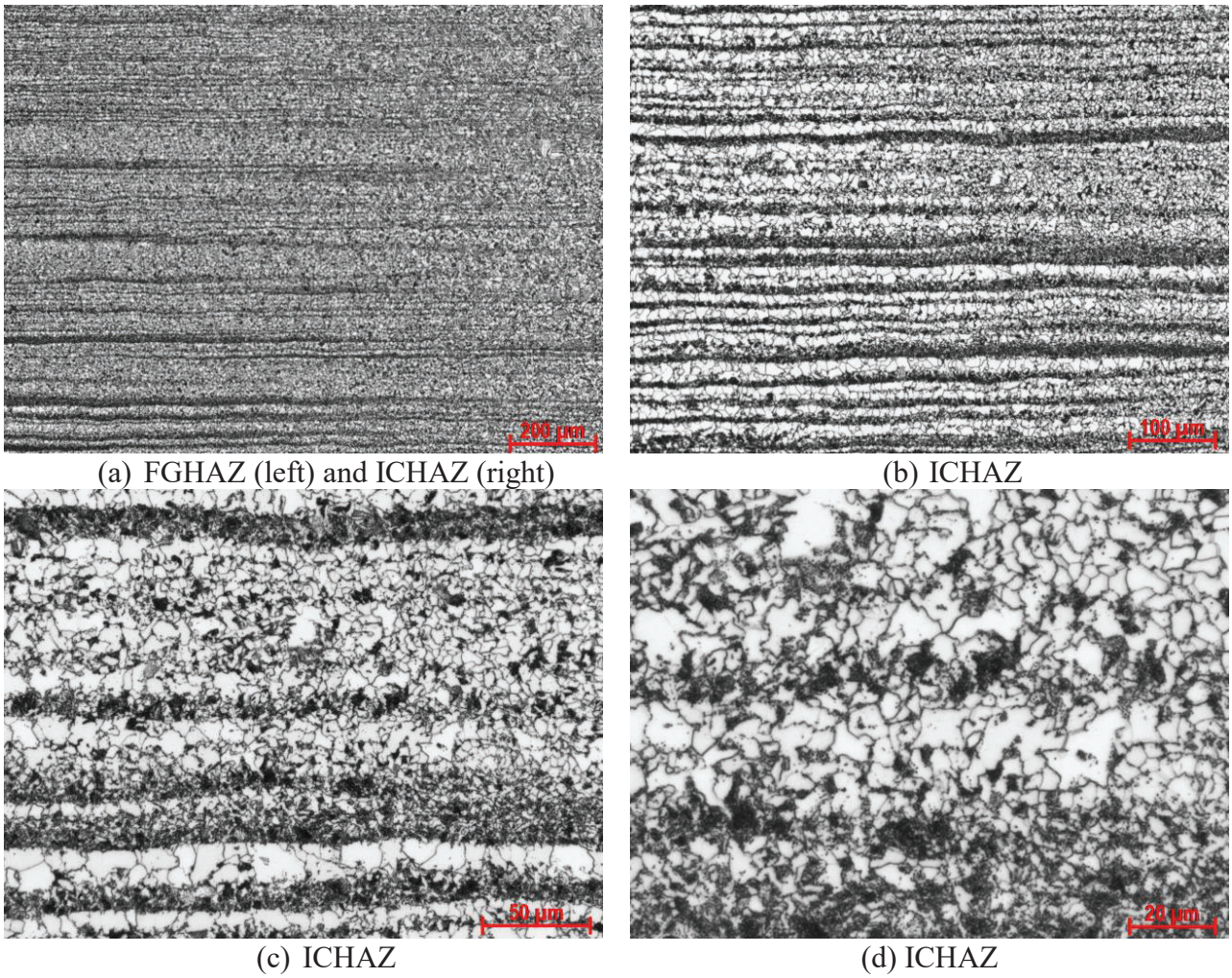

(a) FGHAZ (left) and ICHAZ (right)

(b) ICHAZ

(c) ICHAZ

(d) ICHAZ

Figure 11. Microstructures of IGHAZ close to mid-thickness of the weld region.

3.4 Tensile Properties

According to AAR specification [4], AWM tension tests are used to measure the strength and ductility of the weld metal while cross-weld tension tests (or joint-tension tests) are employed to measure only the strength of the weld joint. In this work, cylindrical cross-weld tension specimens (Figure 2) were used to measure the strength and examine failure characteristics of a current TC128B longitudinal weld joint at different temperatures. For cylindrical tensile specimens, the specimens sampled the mid-thickness portion of the weld, i.e., the second-pass weld metal and some RH-WM. The AAR specification requires that the joint specimen breaks in the BM outside the weld and the strength is not more than 5% below the specified ultimate tensile strength of TC128B (UTS) (i.e., 560 MPa at room temperature) [4].

Two longitudinal AWM tests showed repeatable results. Representative stress-strain curves of the TC128B longitudinal and circumferential AWM [3] and BM [1] specimens are shown in Figure 12. AWM specimens showed higher flow stresses and lower elongation than those of the BM specimen and displayed discontinuous yield up to approximately 1.5-1.7% strain. The strengths of longitudinal

AWM specimens were equivalent to but slightly lower (approximately 2.2%) than those of circumferential AWM specimens which might be due to slightly lower C content in the longitudinal weld.

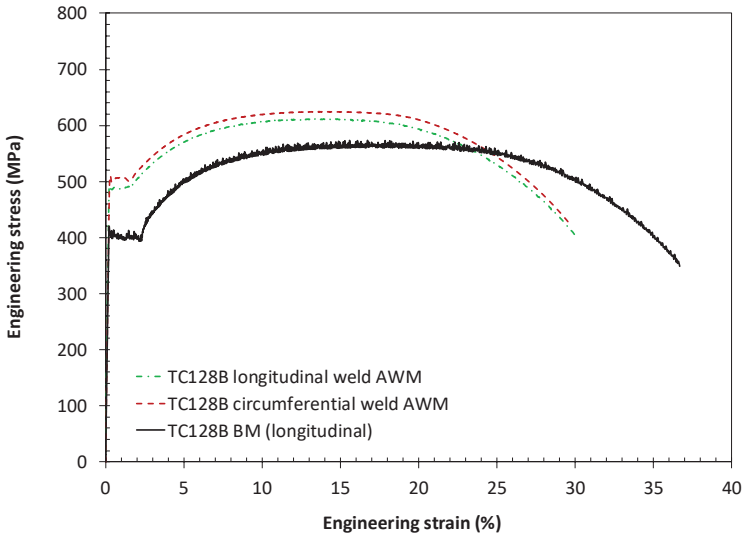

(a) Engineering stress-strain curve

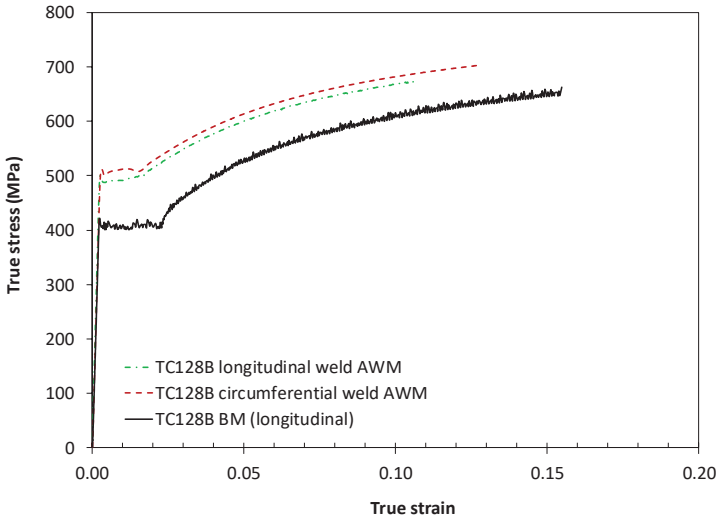

(b) True stress-strain curve

Figure 12. Stress-strain curves of TC128B AWM and BM.

Figure 13 shows nominal stress-strain curves of the weld specimens and that of BM. Longitudinal and circumferential cross-weld tensile specimens (including the full-thickness ones for the circumferential weld [3]) showed shorter discontinuous regions and higher yield strength than the BM. This may be useful for modelling calibration. The strain along the gauge length in a cross-weld tensile specimen is not uniform due to the presence of the hard WM, therefore, the stress-strain curve can only be considered as a nominal stress-strain curve for information and comparison to the BM. (Note that the nominal strains of cylindrical cross-weld tensile specimens were deduced from the machine grips displacement and corrected to match the elastic stress-strain of steel.) When one examines these tensile

stress-strain curves it should also be noted that the rectangular and cylindrical cross-weld tensile specimens had a gauge length of 50 mm, longer than that of the common cylindrical BM specimen of 25 mm [1], and the total failure elongation of a longer gauge-length specimen is usually smaller than that of a shorter gauge length.

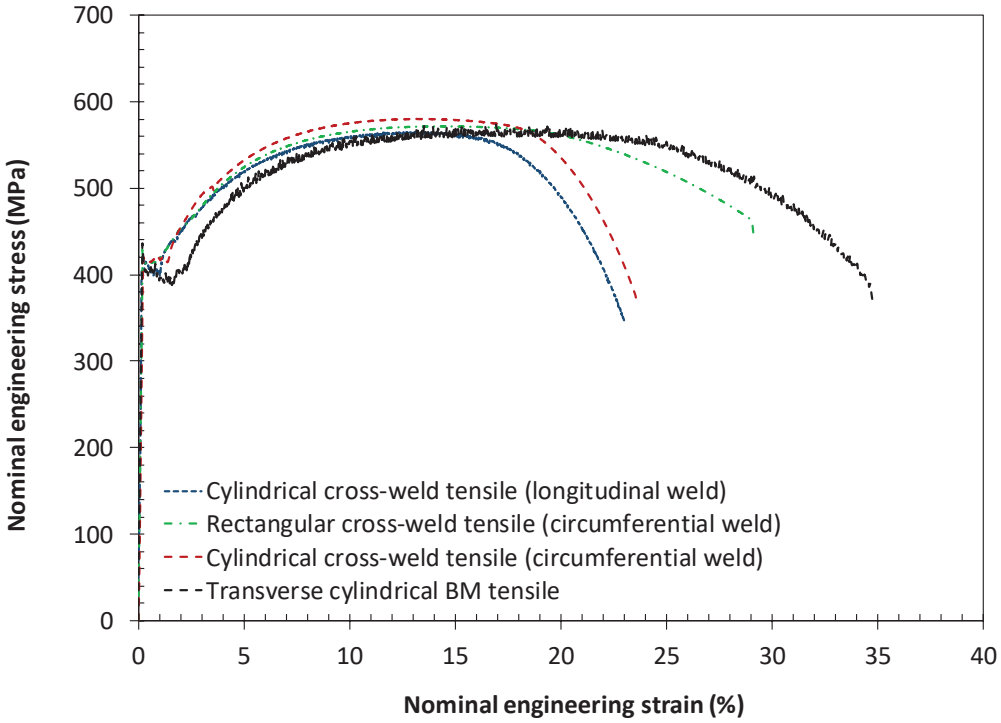

Figure 13. Nominal engineering stress-strain curves of cross-weld specimens.

Tensile test results of TC128B longitudinal weld are summarized in Table 2 including yield strength (σ_y), UTS (σ_{UTS}) and elongation at failure in cylindrical specimens (E.L.); average low-temperature tensile properties of the TC128B BM and two results of the circumferential weld are also provided in Table 2. The UTS of cross-weld specimens increased with decreasing temperature as shown in Figure 14 which is consistent with the dislocation-controlled rate-dependent phenomenon. Photographs of tested tensile specimens are shown in Figure 15. Note that the white lines inserted in Figure 15 are separating WM based on visual observations. All cross-weld specimens tested at 23°C and below failed in the BM. The results show desired WM strength over-match against BM (i.e., WM is stronger than BM).

Table 2. Tensile properties of TC128B steel [1]/circumferential weld [3] and longitudinal weld specimens

Sample	Orientation/Specimen	T (°C) (Specimen #)	σ_y (MPa)	σ_{UTS} (MPa)	E.L. in 25 mm (%)	Failure Location
BM	TD/cylindrical	23 (avg.)	389	573	35	Normal (i.e., within specimen gauge)
	RD/cylindrical	23 (avg.)	390	574	37	
	RD/cylindrical	0 (avg.)	405	589	36	
	RD/cylindrical	-20 (avg.)	416	606	35	
	RD/cylindrical	-40 (avg.)	437	626	37	
	RD/cylindrical	-60 (avg.)	453	654	37	
Circumferential weld	Along circumferential weld/ cylindrical (AWM)	23 (#1)	497	624	27	
		23 (#2)	500	625	30	
Longitudinal weld	Along longitudinal weld/ cylindrical (AWM)	23 (#1)	474	609	30	
		23 (#2)	486	612	31	
	Transverse/cylindrical	23 (#3)	-	562	-	BM
		23 (#4)		558		BM
		23 (#18)		566		BM
		0 (#6)		584		BM
		0 (#7)		586		BM
		0 (#8)		586		BM
		-20 (#9)		599		BM
		-20 (#10)		605		BM
		-20 (#11)		609		BM
		-40 (#12)		629		BM
		-40 (#13)		629		BM
		-40 (#14)		631		BM
		-60 (#15)		657		BM
		-60 (#16)		658		BM
		-60 (#17)		665		BM

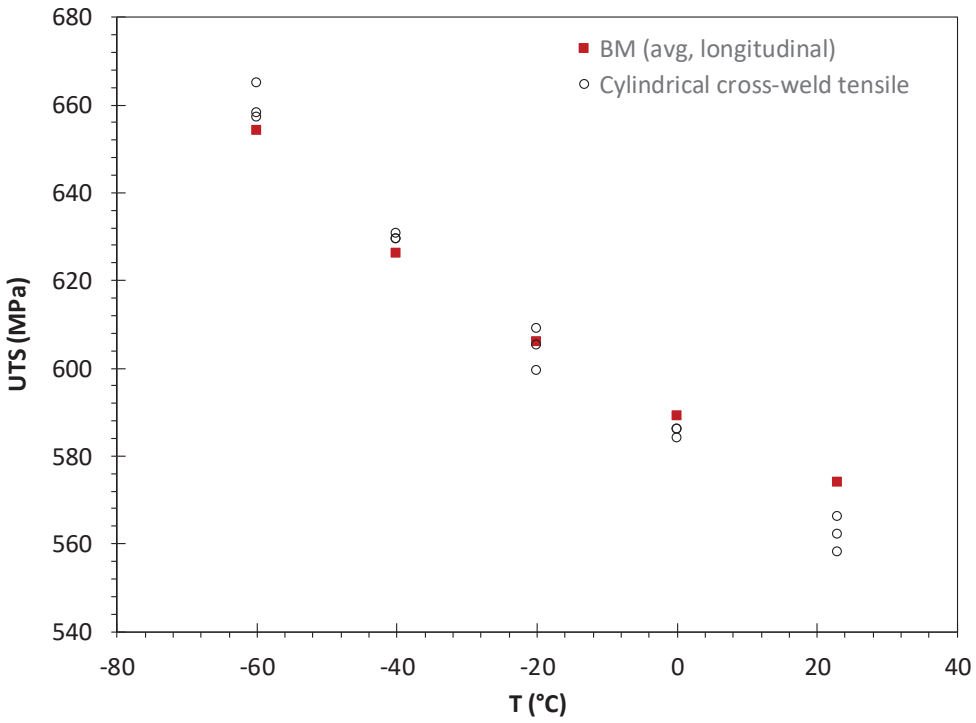

Figure 14. UTS vs. temperature of cross-weld tensile specimens of TC128B longitudinal weld.

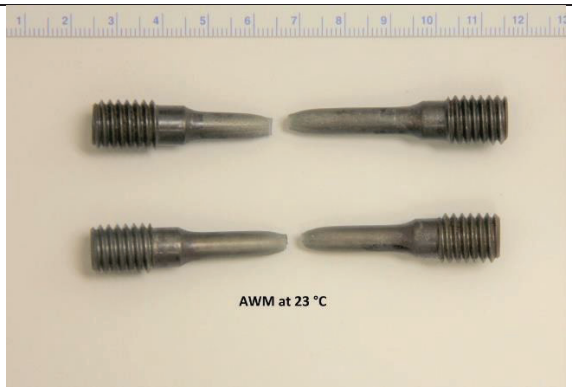

(a) All weld-metal specimens at 23°C

(b) Cross-weld specimens at 23°C

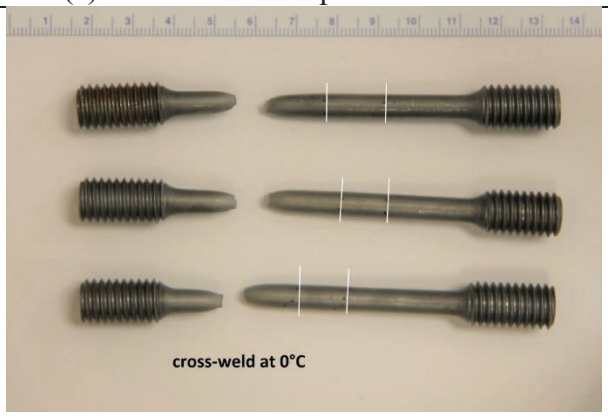

(c) Cross-weld specimens at 0°C

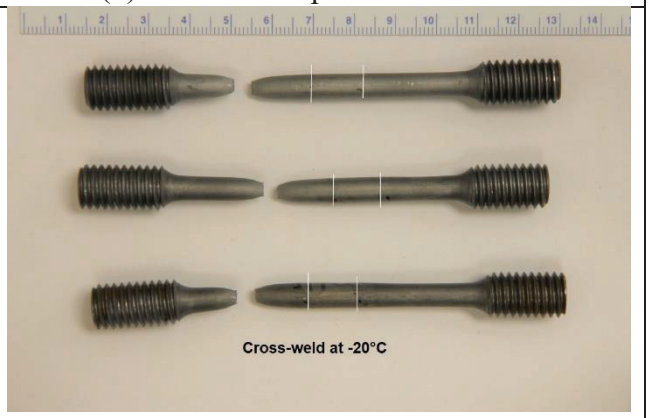

(d) Cross-weld specimens at -20°C

(e) Cross-weld specimens at -40°C

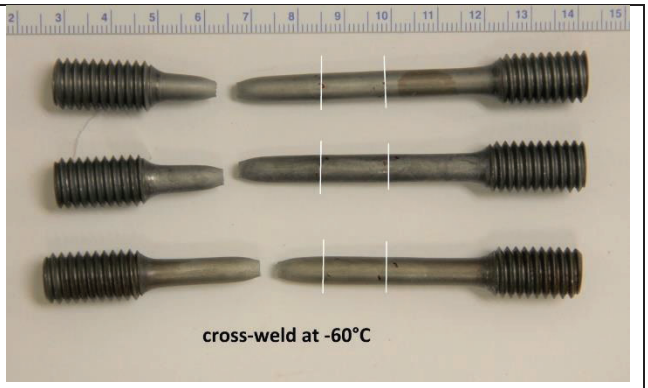

(f) Cross-weld specimens at -60°C

Figure 15. Photographs of cylindrical tensile specimens. White lines indicate the approximate weld region in cross-weld specimens.

3.5 Charpy Impact Properties

Charpy impact toughness is the only toughness requirement included in the AAR tank car steel specifications for pressure tanks. Charpy impact tests are also used to evaluate welding procedures for low-temperature applications [4]. The objectives of this work were (i) to provide experimental Charpy data of the circumferential weld at the benchmark specification temperature (-34 °C), and (ii) to establish Charpy transition toughness curves of a current TC128B longitudinal weld joint and to compare the weld toughness to the base steel and circumferential weld toughness. Testing of the circumferential weld was critical and possible because of available weld material for preparing additional Charpy specimens.

3.5.1 Charpy properties of the circumferential weld at -34 °C

The initial Charpy tests at -34 °C yielded CVN values of 29 J, ***13 J*** and 24 J. The minimum value of one of the three specimens is less than the benchmark required value (i.e., 13.6 J in Appendix W 8.1.4.1) but met the retest requirements as the average of the three specimens (22 J), which is higher than 13.6 J. According to Appendix W 8.1.4.2, a retest of three additional specimens must be made and each of which must be equal to or exceed the specified minimum AAR required value for the average of the three specimens (i.e., 20.3 J). The retest of three specimens yielded CVN values of 20 J, 19 J and 20 J, each of which were lower than the AAR retest requirement of 20.3 J and hence, the toughness of circumferential weld did not meet the benchmark specification requirement although the values were close to the requirements in both tests. CVN results are provided in Table 3 including results obtained in [3]. Charpy transition curves TC128B BM, circumferential WM and HAZ [1,3] with the CVN data at -34°C are shown in Figure 16. The fitting curves are of the form $CVN = C_1 + C_2 \tanh\left(\frac{T - T_0}{C_3}\right)$ (where C_1, C_2, C_3 and T_0 are constants) to guide visual comparison [1].

The result of a single test series can not be used to conclude that the tank car did not meet the benchmark specification at the time of weld qualification and manufacture. However, the results indicate that

Charpy testing is important for tank cars in low-temperature climate applications. If the same TC128B steel is used for pressure cars, that it would have failed the standard.

The Charpy tests of TC128B showed that the weld exceeds the AAR standard requirements at moderate temperatures (> -20 °C). The material's performance at low temperatures, particularly in weld regions, is borderline (-34 °C). Based on these results, future work to research the integrity of tank cars would be well advised to target low temperature weld performance.

Table 3 Charpy absorbed energy (CVN) of TC128B circumferential weld: average (and individual)

T (°C)	CVN (J)	
	WM	HAZ
25	80 (102,69,69)	208 (232,145,248)
-20	26 (20,28,30)	109 (159,92,75)
-34	21 (29,13,24,20,19,20)	*
-46	18 (16,24,13)	32 (16,17,64)
-60	9 (10,9,9)	92 (120,142,152,66,16,53)
-80	6 (5,7,5)	21 (25,33,6)

* The HAZ was not tested at -34 °C.

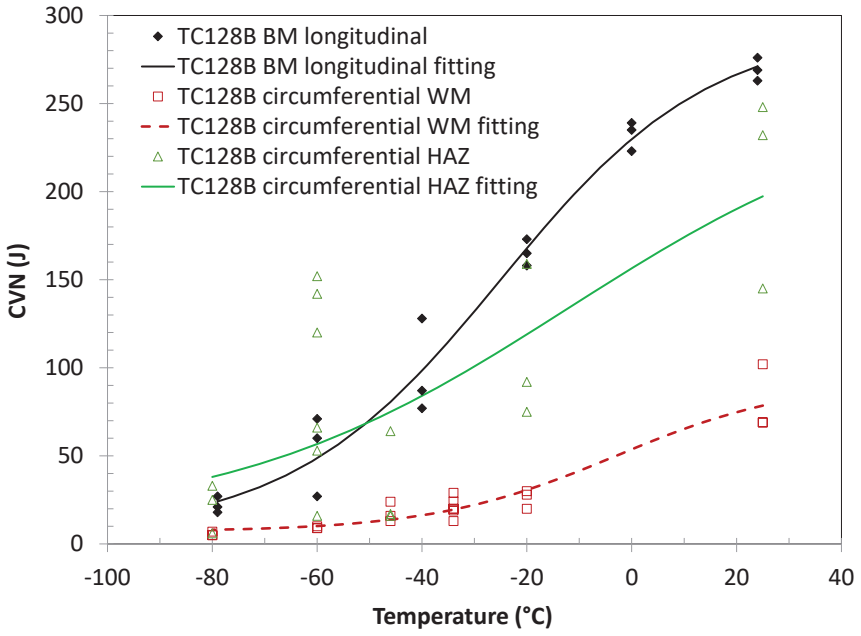

Figure 16 Charpy transition curve of TC128B BM, circumferential WM and HAZ.

3.5.2 Charpy properties of the longitudinal weld

Charpy absorbed energy (CVN) values of TC128B longitudinal weld are given in Table 4. Charpy transition curves including that of the BM are shown in Figure 17. CVN of specimens notched at the HAZs (Figure 5b and Figure 5c) were the highest probably because the specimens sampled a small

portion of HAZ and a large portion of BM which was softened by the welding procedure. CVN of specimens notched at the second-pass weld HAZ showed slightly higher CVN than those notched at the first-pass weld for the longitudinal weld. CVN of the WM were significantly lower than those of the BM and HAZs.

In total, nine WM Charpy specimens were tested at -46°C which is the temperature for specific low temperature applications in the AAR specification (2.1 Special Commodity Requirements) [4]. The DOT-117 tank car that the TC128B for this work originated from is not designed for the special commodity requirements and the results at -46°C should not be considered a failure of the standard. Note that the AAR specification requires a test temperature of -34°C for the DOT-117 tank car used in this research for Charpy toughness testing, however, the testing scheme for this project was modelled after previous years testing which utilized the -46°C test point. For 10×10mm specimens tested at -46°C, the average CVN of the first three tests was 21 J and the minimum value was 14 J; these values would just meet the AAR specification requirement. The second three Charpy tests at -46°C showed significantly lower CVN of the longitudinal WM than the requirement. In order to confirm the results, three additional Charpy WM specimens were prepared from a different location from that of the first six specimens. The results showed that CVN of the longitudinal weld would not meet the specification if the test temperature was -46°C.

Charpy transition curves of the TC128B circumferential and longitudinal WM are compared in Figure 18. The longitudinal WM had comparable CVN at temperatures at and below -46°C but the longitudinal WM had higher CVN than those of the circumferential WM at higher temperatures. This may be due to slightly higher carbon (C) and oxygen (O) contents of the longitudinal weld than those of the circumferential weld. Upper-shelf CVN value decreased with increasing WM oxygen content [14,15]. The Charpy transition curves were fitted to a tanh function which is commonly used to empirically fit CVN data. At the AAR specification requirement temperature of -34°C (AAR Appendix W [4]), the average CVN from interpolation fitting for the longitudinal welds was 30 J. This indicated that CVN of the longitudinal weld met the AAR specification (average 20.3 J). No testing was done at -34°C because no weld material remained.

Table 4 Charpy absorbed energy (CVN) of TC128B longitudinal weld: average (and individual)

T (°C)	CVN (J)		
	WM	HAZ (notched at the second-pass weld)	HAZ (notched at the first-pass weld)
21	109 (112,120,95)	-	225 (216,241,218)
-20	49 (50,53,43)	165 (172,158)	162 (175,165,145)
-46	16 (31,18,14,9,16,13,12,16,13)	121 (125,123,114)	109 (98,110,118)
-60	11 (9,17,8)	-	88 (69,95,99)
-80	5 (4,4,6)	-	21 (23,19,22)

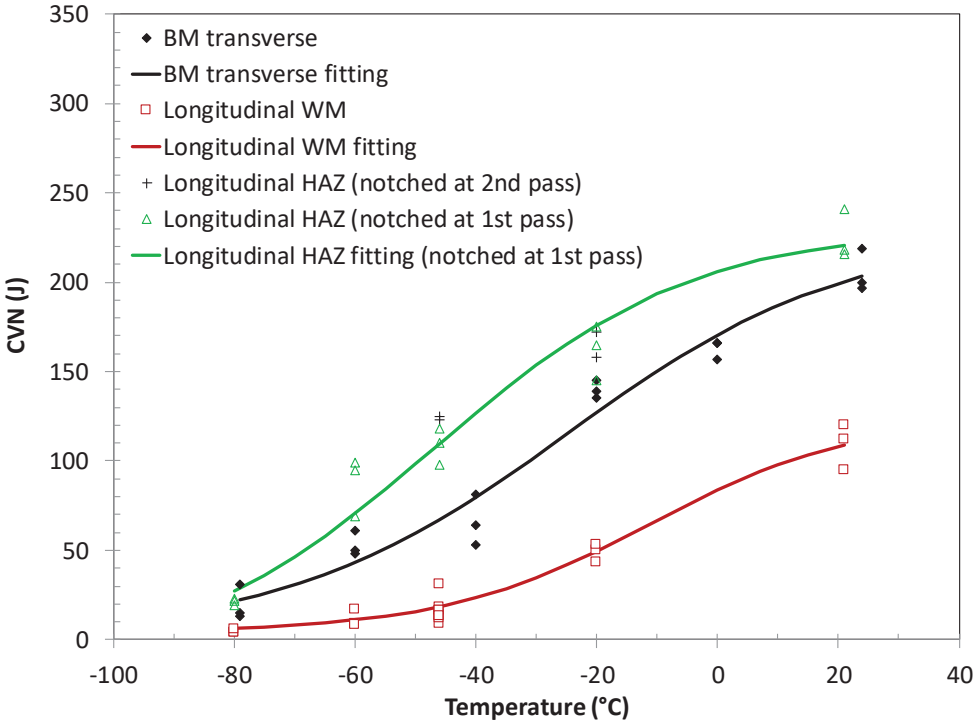

Figure 17. Charpy transition curve of TC128B BM, longitudinal WM and HAZs.

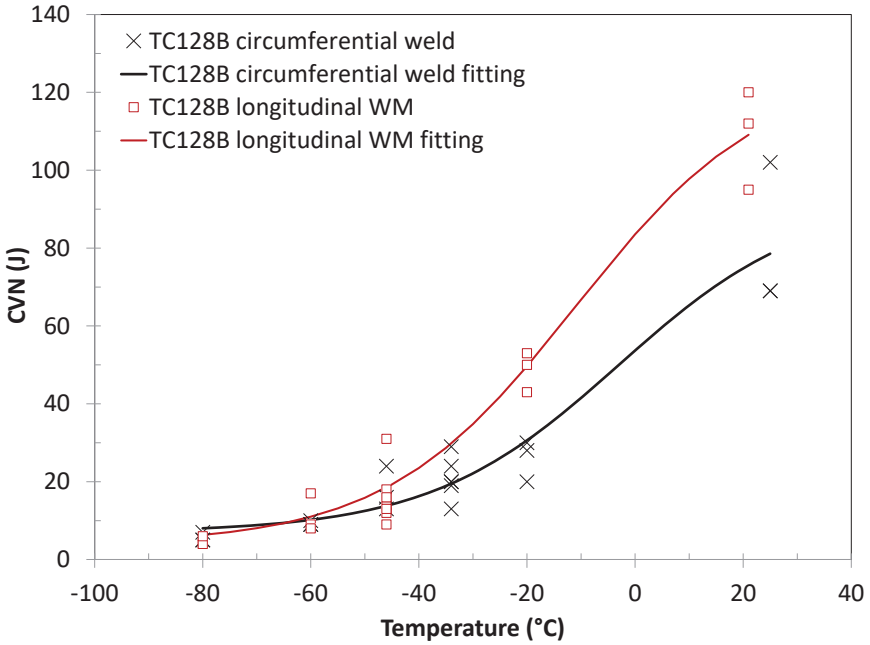

Figure 18. Charpy transition curve of TC128B circumferential and longitudinal WM.

4. DISCUSSION ON WELD METAL TOUGHNESS

This discussion section is focused on low TC128B weld Charpy toughness including fracture features, mechanism, possible causes and remedies.

4.1 SEM Fractography of TC128B Circumferential WM Charpy Specimens

The aims of fractographic examination were to examine typical fracture features and fracture mechanism of low CVN WM samples. Fracture surfaces of two TC128B circumferential weld metal (WM) Charpy specimens were examined, one tested at 25°C with CVN=69 J and another tested at -46°C with CVN=13 J. Both specimens had the lowest CVN at the test temperatures and displayed mainly brittle fracture features.

Both specimens showed cleavage fracture after limited or minimum ductile fracture. The specimen with CVN=69 J showed approximately 35% shear lips (ductile) and 65% brittle (crystallinity) fracture; in the brittle fracture initiation region, isolated ductile fracture areas could be seen with cleavage fracture. This would be expected because of the observed low CVN. The cleavage initiation regions in the two specimens could be identified and no weld flaws were observed (Figure 19 and Figure 20). The specimen with CVN=13 J displayed cleavage fracture. Many round-shape inclusions were observed in voids in the ductile fracture region (Figure 19d). The inclusions are likely oxides although the composition of inclusions was not determined. Note that low WM toughness in steel welds may also be related to welding defects or flaws [e.g., 16,17]. The SEM fractography examinations indicate that low TC128B WM toughness was associated with weld microstructural constituents and/or inclusions but not weld flaws. Hence, it is unlikely low weld toughness was caused by poor weld flaws.

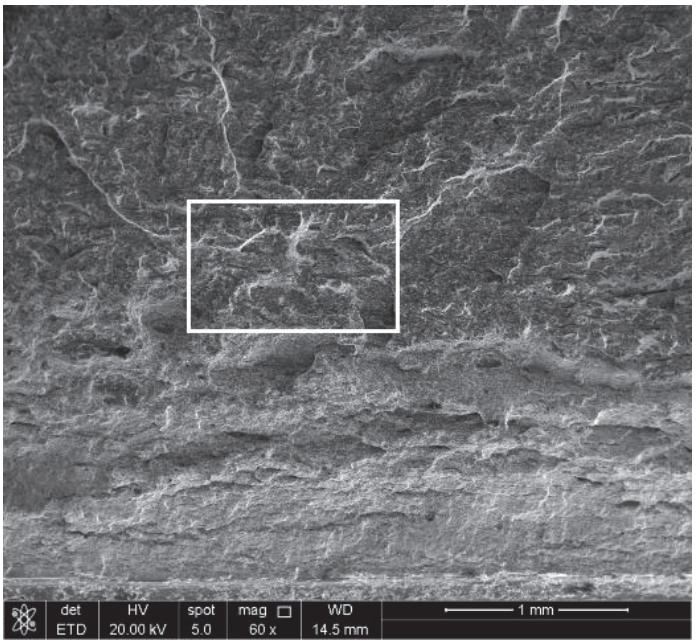

(a) Cleavage fracture initiation region after approximately 1.2 mm ductile fracture extension

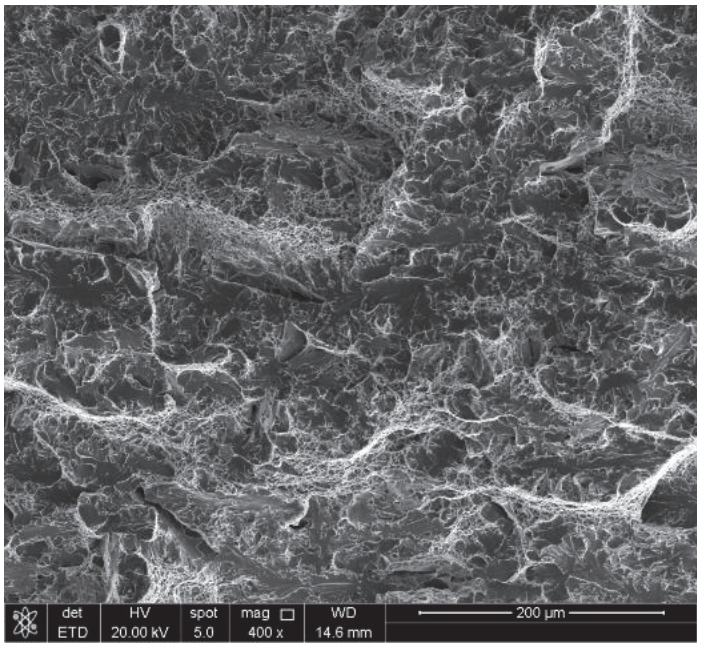

(b) Close-up view of cleavage initiation region

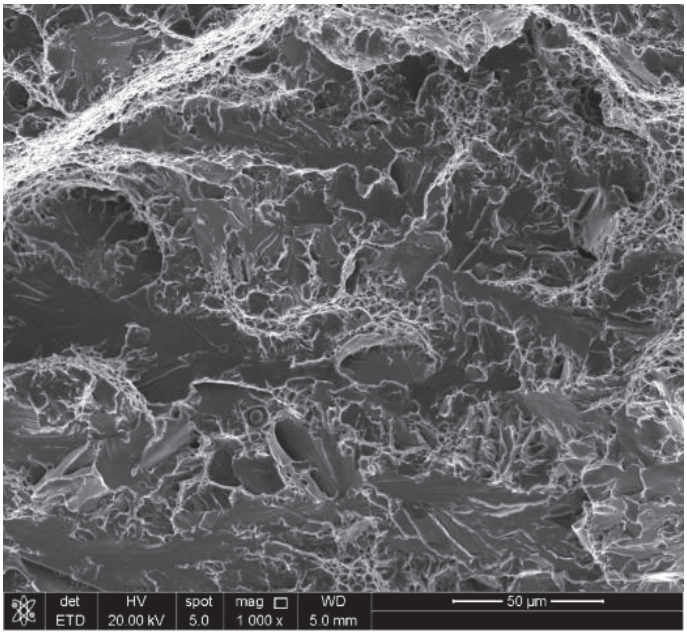

(c) Cleavage fracture close to initiation

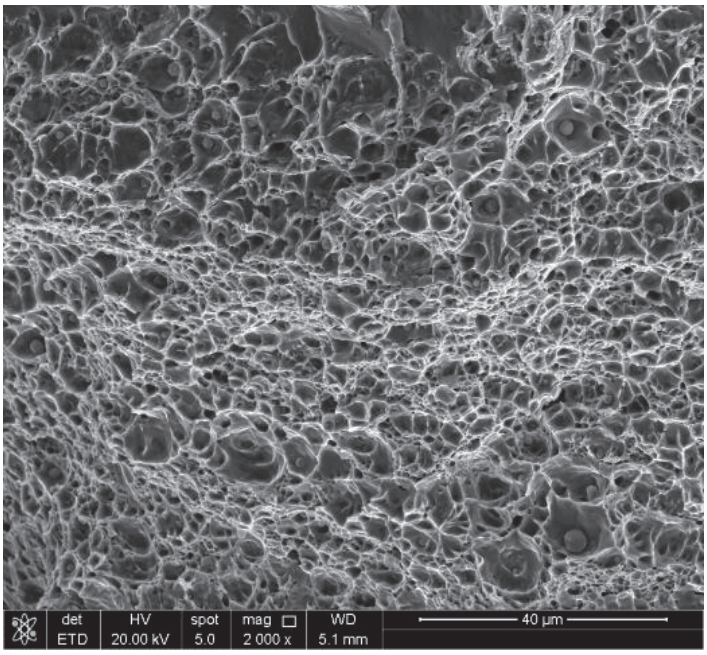

(d) Ductile fracture close to cleavage initiation region showing many round inclusions in voids

Figure 19 SEM fractographs of Charpy WM specimen tested at 25°C with CVN=69 J (W2 specimen).

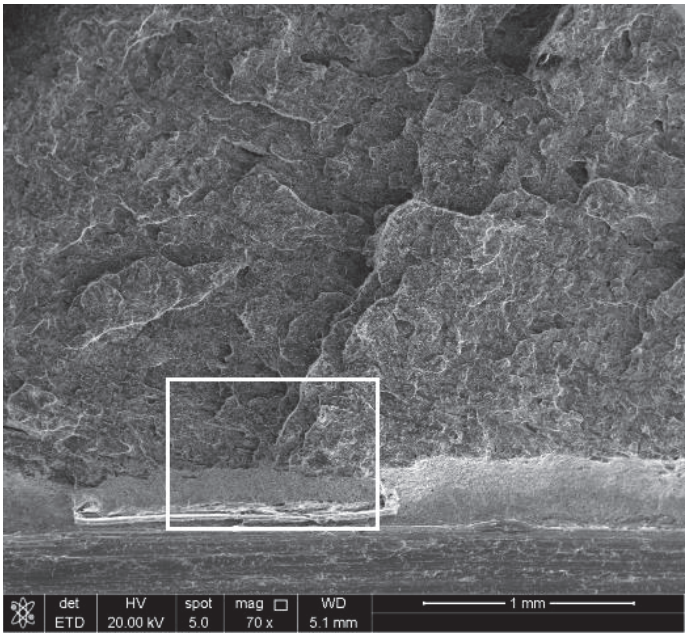

(a) Cleavage fracture initiation region after approximately 0.2 mm ductile fracture extension

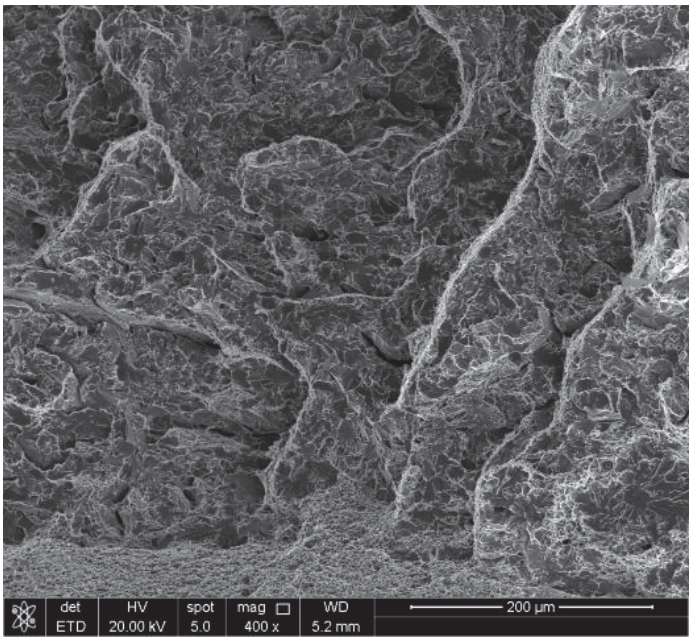

(b) Close-up view of cleavage initiation region

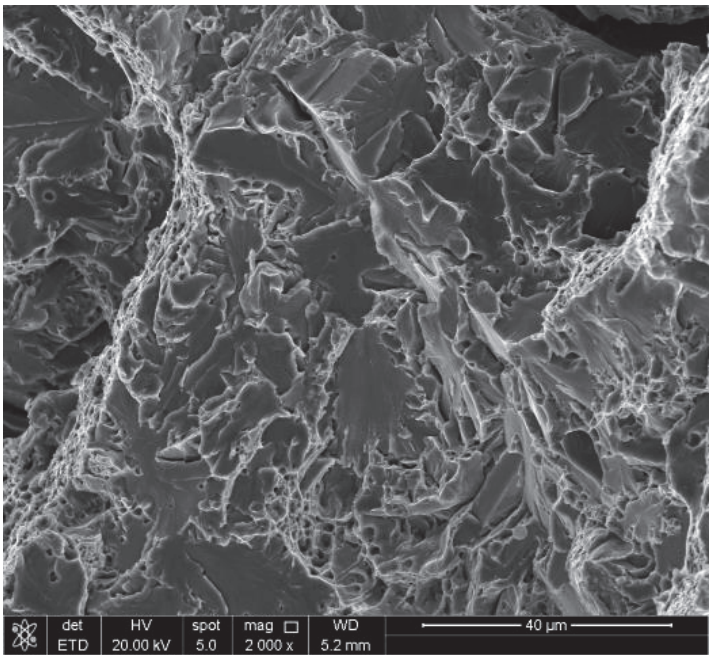

(c) Cleavage fracture in the initiation region

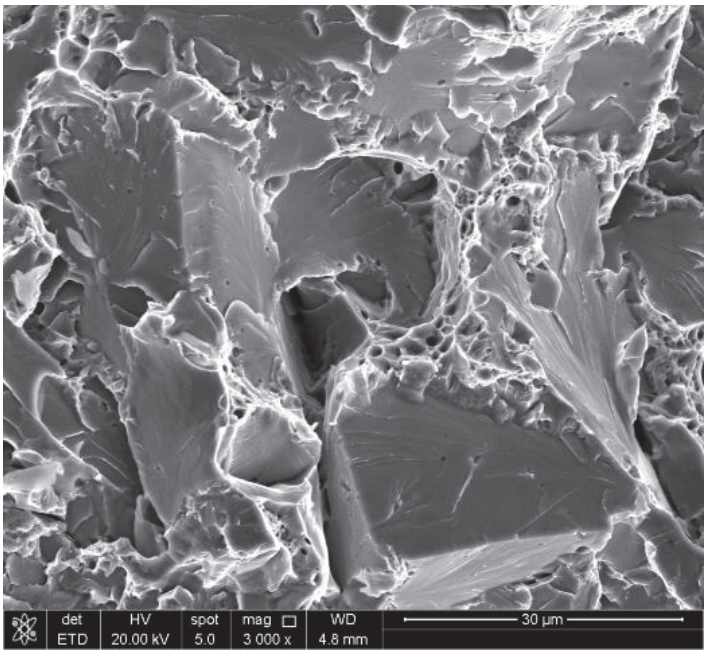

(d) High magnification fractograph of cleavage fracture initiation region

Figure 20 SEM fractographs of Charpy WM specimen tested at -46°C with CVN=13 J (W9 specimen).

4.2 Acicular Ferrite Formed in TC128B Weld

As revealed by optical microscope and scanning electronic microscope, the WM consisted of a large quantity of coarse grain boundary ferrite, some intergranular polygonal ferrite, and ferrite with second phase, as well as a small volume percentage of AF. It has been reported that the formation of AF and its volume percentage are important to the toughness of the weld [13,15]. Acicular ferrite nucleates heterogeneously on the surface of non-metallic inclusions in the weld metal during the austenite-ferrite-transition. As transformation continues, the ferrite grains radiate in various directions, creating a chaotic construction of crystallographically disoriented plates of approximately 5-15 μm in length and 1-3 μm in width. Thereby, the typical fine-grained and interlocking structure of AF is formed. Compared with other microstructural constituents, it is much more difficult for cleavage cracks to propagate across this chaotically-oriented interlocking structure, which leads to a significant increase in mechanical properties, most notably in toughness.

Quantitative analysis of microstructure formed in the weld metal has crucial importance due to the effect of phase-type, amount, distribution and morphology on final mechanical properties. Typically, it has been reported that the formation of AF and its volume percentage is important to the toughness of the weld. Consequently, quantitative analysis of microstructure was carried out in this work using an image analysis method, described as follows.

First, three optical microstructure images were randomly taken from the center region of the weld metal of the second pass at a magnification of 500 times. Then the regions of different microstructures were outlined and marked with different colors, as shown in Figure 21, as an example. Finally, the percentage

of those different microstructures were determined by an image analysis software. Quantitative analysis of microstructure showed that the weld metal contained approximately 40% AF, 36% coarse grain boundary ferrite (GBF) as well as 21 % intragranular polygonal ferrite (PF(I)) and ferrite with the aligned second phase (FS(A)). The volume percentage of AF formed in the TC128B circumferential WM was estimated to be around 25% by image analysis. As a result, the limited formation of AF may be the main reason leading to low CVN. The formation of AF is mainly affected by weld metal composition, cooling rate, inclusion landscape and austenite grain size. In order to improve the toughness of TC128B weld metal, the current welding procedure needs to be modified or a new welding procedure needs to be developed in order to optimize the formation of AF.

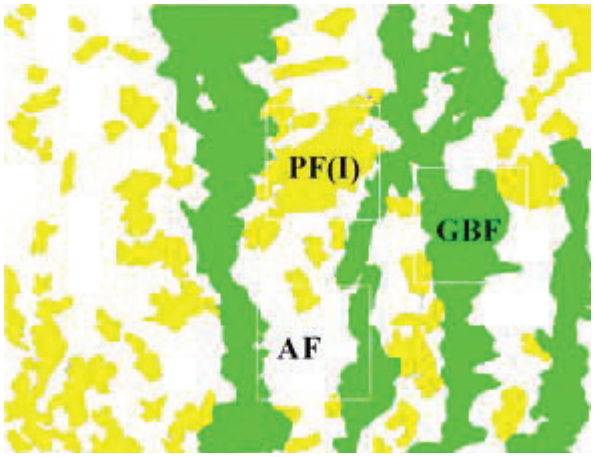

Figure 21 Illustration of areas with different microstructures of longitudinal weld for imaging analysis.

In summary, the low CVN of the circumferential weld may be due to high carbon and oxygen contents, and coarse proeutectoid ferrite and less AF (approximately 25%) than the usual similar welds [13]. Other possible reasons include that welding procedure specification (WPS) of SAW gives only marginal toughness over the required toughness, variations in welding parameters during the welding operation, filler wire and flux composition changes, and moisture control. Since oxygen content above 0.055% (550 ppm) generates many oxide inclusions [6], the oxygen level of 0.0559% of the weld can provide many potential cleavage initiation sites from oxides partially responsible for the observed low CVN.

Although the longitudinal weld contains more AF and hence shows a higher CVN than the circumferential weld does (Figure 18), the CVN energy of the WM is much lower than that of the BM across all temperatures, as shown in Figure 17. This means that in an accident involving impact the weld is most likely the failure location. It should be noted that the results were from one tank car. Improving the toughness of the weld metal would reduce the chance of fracture/rupture under all service conditions. Weld toughness can be improved by adjusting the welding process, the filler metal, reducing heat/current, argon shielding, and the post-weld heat treatment.

5. RECOMMENDED FUTURE WORK

The following areas are recommended for further work based on the results obtained in this project.

- Experimentally establish Charpy ductile-to-brittle transition curve for other tank car welds if material is available to determine whether low weld toughness is an isolated or systemic issue.
- Establish Charpy and fracture toughness correlation of tank car SAW seam welds for Engineering Critical Assessment (ECA). The objective is to generate a database of Charpy and fracture toughness values of tank car welds at toughness level close to the specification required values for engineering critical assessment (ECA).
- Investigate current industry standard weld practices and develop improvement/suggestions
- Determine effects of pre-deformation on properties for TC128B or A516-70 plate (e.g., deformation during forming operation).
- Obtain tank car steels from at least two other sources of TC128B and other tank car steels (e.g., ASTM A572 Grade 50 Type 2) to obtain a comprehensive dataset.
- Investigate locations of crack initiation and failure in tank cars. Determine whether welds are common crack initiation sites.

CONCLUSIONS

Circumferential and longitudinal welds from a new tank car manufactured with TC 128B were characterized and tested. The main findings are summarized below.

- The welds were produced with a double pass procedure. The first-pass (or root pass) weld was made from the inside of the tank and the WM height was about 1/3 of the weld thickness while the second-pass (or cap pass) weld completed the joints. For the two welds, the combined weld and HAZ widths were approximately 14.8-19.8 mm close to the mid-thickness (the smallest). The HAZ width ranged approximately 1.3-5.7 mm.
- WM and HAZ showed typical microstructures although AF volume was low.
- The micro-hardness values (H_v) in the weld and HAZ were considerably higher than those of BM, i.e., demonstrating desired weld strength over-matching (i.e., WM was stronger than BM). The hardness values of the two welds were comparable. The average values of micro-hardness of BM, HAZ and WM of the two welds were 164, 191 and 201, respectively.
- All-WM specimens tested at 23°C showed that the welds were manufactured to the strength specification.
- The UTS of cross-weld specimens increased with decreasing temperature from 850°C to -60°C. All cross-weld specimens tested failed at BM except for two cross-weld tensile specimens at 800°C failed at WM although they failed at similar stresses [3].
- CVN values of WM were significantly lower than those of BM and HAZs specimens. CVN values for circumferential WM specimens at -34°C showed that the circumferential weld toughness values did not meeting the benchmark of AAR specification requirements for pressure tanks (i.e., average of 20.3 J and minimum of 13.6 J).
- The SEM fractography examinations indicate that low TC128B WM toughness was associated with weld microstructural constituents and/or inclusions.

- The volume fractions of AF in the circumferential and longitudinal welds were estimated to be 25% and 40%, respectively. In order to improve the toughness of TC128B weld metal, the current welding procedure needs to be modified or a new welding procedure needs to be developed in order to optimize the formation of AF. The low AF volume fraction was generally considered to associate with low CVN.

ACKNOWLEDGEMENTS

This work was funded by Transport Canada's Transportation of Dangerous Goods Directorate under the guidance of Mr. Michael Spiess, Mr. Ian Whittal and Mr. Henry Lu. Mr. Michael Spiess, Mr. Ian Whittal, Mr. Henry Lu and Mr. Shaun Singh are gratefully acknowledged for very helpful review of the report. We would like to gratefully acknowledge Mr. S. Amey for sample preparation, Ms. R. Zavadil and Ms. P. Liu for performing metallography and micro-hardness.

REFERENCES

1. S. Xu, J. Liang, L. Yang, A. Laver and W.R. Tyson, “Tensile and Fracture Toughness of a Current Tank Car Steel, TC128B”, CanmetMATERIALS Report, CMAT-2017-WF 16144032, May 2017.
2. C.H.M. Simha and J. Mckinley, “High-Temperature Mechanical Properties of Tank Car Steel – Testing and Analysis”, CanmetMATERIALS Report, CMAT-2017-WF 15390827, November 2017.
3. S. Xu, J. McKinley, J. Chen, J. Liang and A. Laver, “Characterization of Microstructure, Tensile (23°C to 850°C) and Charpy Transition Curves of a Current Tank Car Steel (TC128B) Circumferential Weld”, CMAT-2018-WF 34540443, January 2019.
4. AAR Manual of Standards and Recommended Practices, Section C-III (Appendix M, M-1002, and Annex W), “Specifications for Tank Cars”, 2014.
5. ASTM A20/A20M-15, “Standard Specification for General Requirements for Steel Plates for Pressure Vessels”, ASTM International, 100 Barr Harbor Drive, PO Box C700, West Conshohocken, PA 19428-2959, United States, November 2015.
6. J. Amanie, “Effect of Submerged Arc Welding Parameters on the Microstructure of SA516 and A709 Steel Welds”, PhD Thesis, Department of Mechanical Engineering, University of Saskatchewan, Saskatoon, Canada, August 2011. (https://harvest.usask.ca/bitstream/handle/10388/ETD-2011-07-42/AMANIE-DISSERTATION.pdf?sequence=3&isAllowed=y)
7. M.A. Sutton, I. Abdelmajid, W. Zhao, D. Wang and C. Hubbard, “Weld Characterization and Residual Stress Measurements for TC-128B Steel Plate”, Journal of Pressure Vessel Technology, Vol. 124, 2002, pp. 405-414.
8. J.A. Gianetto, D.M. Mak, R. Bouchard, S. Xu, and W.R. Tyson, “Characterization of the Microstructure and Toughness of DSAW and ERW Seam Welds of Older Linepipe Steels”, Proc.4th International Pipeline Conference (IPC2002), Calgary, Alberta, Canada, Sept. 29-Oct. 4, 2002, ASME, Paper IPC02-27157, pp.1-12.
9. J.A. Francis, W. Mazur and H.K.D.H. Bhadeshia, “Review Type IV Cracking in Ferritic Power Plant Steels”, Materials Science and Technology, Vol. 22, 2006, pp. 1387-1395

10. S. L. Mannan and K. Laha, “Creep-Behavior of Cr-Mo Steel Weldments”, Transactions of the Indian Institute of Metals, Vol. 49, 1996, pp. 303–320.
11. G.E. Hicho, “The Mechanical, Stress-Rupture, and Fracture Toughness Properties of Normalized and Stress Relieved AAR TC128 Grade B Steel at Elevated Temperatures”, Report NISTIR 5157, March 1993.
12. G.E. Hicho and D.E. Harne, “Weld and Heat Affected Zone Crack Arrest Fracture Toughness of AAR TC128 Grade B Steel”, NISTIR 4767, Report No. 25, NIST, February 1992.
13. L.E. Svensson and B. Gretoft, "Microstructure and Impact Toughness of C-Mn Weld Metals", Welding Research Supplement, December 1990, pp. 454-s - 461-s.
14. D.J. Abson and R.J. Pargeter, “Factors Influencing As-deposited Strength, Microstrucutre, and Toughness of Manual Metal Arc Welds Suitable for C-Mn Steel Fabrications”, International Metals Reviews, Vol. 31, 1986, pp. 141-194.
15. L. Devillers, D. Keplan, B. Marandet, A. Ribes and P.V. Ribond, “The Effect of Low Level of Some Elements on the Toughness of Submerged- Arc Welded CMn Steel Welds”, Int. Conf. Proc. The Effects of Residual, Impurity and Microalloying Elements on Weldability and Weld Properties, Abington, The Welding Institute, 1984, Paper 1.
16. Wei Shitong, Lu Shanping, Li Dianzhong and Li Yiyi, “ Impact Property Analysis of Weld Metal and Heat-Affected Zone for Low-alloy Carbon Steel Multi-pass Welded Joint”, China Welding, Vol. 19, No. 1, March 2010, pp. 21-25.
17. S. Xu, J.A. Gianetto, W.R. Tyson and S. Matsuno, “Toughness of EW Pipe Seam Welds: Fractography and Fracture Path Observations on Charpy-V-Notch Impact Specimens from Contemporary Pipe Steels”, *Journal of Pipeline Engineering (incorporating the Journal of Pipeline Integrity),* Vol. 17, No. 3, 2018, pp. 211-224 (Special Issue on ERW Toughness and Integrity).